

submitted to *The Astrophysical Journal*

On the Submillimeter Opacity of Protoplanetary Disks

B. T. Draine

Princeton University Observatory, Peyton Hall, Princeton, NJ 08544;
draine@astro.princeton.edu

ABSTRACT

Solid particles with the composition of interstellar dust and power-law size distribution $dn/da \propto a^{-p}$ for $a \leq a_{\max}$ with $a_{\max} \gtrsim 3\lambda$ and $3 < p < 4$ will have submm opacity spectral index $\beta(\lambda) \equiv d \ln \kappa / d \ln \nu \approx (p-3)\beta_{\text{ism}}$, where $\beta_{\text{ism}} \approx 1.7$ is the opacity spectral index of interstellar dust material in the Rayleigh limit. For the power-law index $p \approx 3.5$ that characterizes interstellar dust, and that appears likely for particles growing by agglomeration in protoplanetary disks, grain growth to sizes $a \gtrsim 3 \text{ mm}$ will result in $\beta(1 \text{ mm}) \lesssim 1$. Grain growth can naturally account for $\beta \approx 1$ observed for protoplanetary disks, provided that $a_{\max} \gtrsim 3\lambda$.

Subject headings: planetary systems: protoplanetary disks dust, extinction, submillimeter

1. Introduction

From mm to mid-infrared wavelengths, the radiation emitted by protoplanetary disks is primarily due to thermal emission from solid particles, just as for the interstellar clouds out of which the protostars form. If the emitting medium is optically thin, then the observed flux density F_ν is proportional to the mass M_d of emitting particles,

$$F_\nu \approx \kappa(\nu) M_d B_\nu(T_d) d^{-2} \quad , \quad (1)$$

where $\kappa(\nu)$ and T_d are the opacity and temperature of the solid material, B_ν is the blackbody intensity, and d is the distance. At submm wavelengths, the Rayleigh-Jeans limit $h\nu \ll kT_d$ usually applies, and

$$F_\nu \approx \frac{2k}{c^2} \nu^2 \kappa(\nu) \frac{M_d T_d}{d^2} \quad (2)$$

is proportional to the product $M_d T_d$. If T_d can be estimated from the observed spectrum or other considerations, the observed F_ν allows M_d to be determined, provided that κ and d are known.

If the opacity has a power-law dependence on frequency, $\kappa(\nu) \propto \nu^\beta$, the observed flux $F_\nu \propto \nu^\alpha$, with $\alpha = 2 + \beta$. Even if the absolute opacity cannot be determined, multiwavelength observations allow the opacity spectral index $\beta(\lambda) \equiv d \ln \kappa / d \ln \nu$ to be measured.

Observations of the infrared and submm emission from diffuse interstellar clouds (with masses estimated independently from observations of H I and CO) allow the opacity κ of interstellar dust to be determined. The observed far-infrared and submm emission from diffuse clouds is consistent with $\beta \approx 1.7$ (Finkbeiner, Davis, & Schlegel 1999; Li & Draine 2001).

The opacity spectral index β can also be determined for dust in dense molecular clouds. The dust near embedded infrared sources in the Orion ridge has $\beta \approx 1.9$ between $1100\mu\text{m}$ and $450\mu\text{m}$ (Goldsmith, Bergin & Lis 1997). The dust in and around 17 ultracompact H II regions studied by Hunter (1998) has $\beta \approx 2.00 \pm 0.25$ between 350 and $450\mu\text{m}$. Friesen et al. (2005) find $\beta = 1.6^{+0.5}_{-0.3}$ for the dust in 3 hot molecular cores, with densities $n_{\text{H}} \approx 10^8 \text{ cm}^{-3}$. The dust in both diffuse clouds and dark clouds thus appears to be consistent with an opacity spectral index $\beta_{\text{ism}} \approx 1.8 \pm 0.2$ in the submm.

If the dust in protoplanetary disks were both optically thin and similar to interstellar dust, we would expect $\alpha = 2 + \beta_{\text{ism}} \approx 3.8 \pm 0.2$. However, Beckwith and Sargent (1991) found that protoplanetary disks usually have spectra with $2 < \alpha < 3$. The opacity spectral index β_{disk} was estimated by fitting simple disk models; the 24 objects studied had a median $\beta_{\text{disk}} = 0.92$, with $2/3$ of the sample falling in the interval $\beta_{\text{disk}} = 0.9 \pm 0.7$.

Numerous subsequent studies have also found $\beta_{\text{disk}} < \beta_{\text{ism}}$. Natta et al. (2004) find a median $\beta_{\text{disk}} = 0.7$ for a sample of 9 disks around Herbig Ae stars observed with the VLA. Submm interferometry of a rotating disk in the star-forming region IRAS 18089-1732 indicates $\alpha - 2 \approx 3.2$ in the outer envelope, with small-scale structure having $\alpha - 2 \approx 0.5$ (Beuther et al. 2004). Andrews & Williams (2005) obtained submm SEDs for 44 protoplanetary disks in Taurus-Auriga, and found that they can be fit using disk models with $\beta_{\text{disk}} \approx 1$.

There are several possible explanations for the difference between β_{ism} and β_{disk} :

1. Some of the emission may come from regions that are not optically thin, even at mm wavelengths. This appears to be part of the explanation, but radiative transfer models also require material with $\beta_{\text{disk}} \approx 1$ in order to reproduce the observed spectra (e.g., Beckwith & Sargent 1991; Natta et al. 2004; Natta & Testi 2004; Andrews & Williams 2005).
2. The chemical composition of the particles in the disk might be very different from the composition of interstellar grains.
3. Growth by coagulation in protoplanetary disks might lead to “fluffy” structures, with the difference between β_{ism} and β_{disk} being due to differing grain geometry.
4. As has been proposed by a number of authors (e.g., Beckwith & Sargent 1991; Miyake & Nakagawa 1993; D’Alessio et al. 2001; Natta et al. 2004; Natta & Testi 2004) grain growth might have put an appreciable fraction of the solid mass into particles that are so large that they are not in the Rayleigh limit, even at mm wavelengths, leading to reduced β .

Here we show that power-law size distributions $dn/da \propto a^{-p}$ for $a \leq a_{\max}$, with $3 < p < 4$ and $a_{\max} \gtrsim 3\lambda$, will lead to opacity spectral index $\beta \approx (p-3)\beta_s$, where β_s is the opacity spectral index of the solid material in the Rayleigh limit. Therefore, starting with material with the observed $\beta_s \approx 1.7$ of interstellar dust, grain growth with the likely power-law index $p \approx 3.5$ will produce a mixture of sizes with $\beta \approx 0.9$ if $a_{\max} \gtrsim 3\lambda$. Since grain growth is expected to be rapid in protoplanetary disks (e.g., Beckwith et al. 2000; Dullemond & Dominik 2005), this can naturally explain $\beta \approx 1$ observed for protoplanetary disks, without need to appeal to changes in composition or grain geometry, other than size.

We briefly review what is expected regarding the optical constants of candidate materials at submm wavelengths in §2, and conclude that changes in composition are not likely to account for the low β values in disks. Particle size distributions are briefly reviewed in §3, to motivate the adopted power-law distribution. In §4, the opacity is estimated analytically for power-law size distributions, to find the expected behavior. In §5 we calculate the opacity numerically for several candidate materials. Although the dependence on size and wavelength can be complicated for conducting materials (in particular, amorphous carbon), we can reproduce the observed $\beta_{\text{disk}} \approx 1.0$ for candidate materials with very different optical constants. Our results are discussed in §6 and summarized in §7.

2. Dielectric Functions: What is Expected for β_s ?

Let $\beta_s(\lambda) \equiv d \ln \kappa / d \ln \nu$ in the small-particle limit, where κ is the absorption cross section per unit mass of solid material. Simple models of insulators and simple models of conductors both have $\beta_s = 2$ at low frequencies (Draine 2004). How do real materials behave at submm wavelengths?

If the low values of β observed in protoplanetary disks are to be produced by materials with small values of β_s , this would require materials with enhanced low-frequency absorption. In insulators, this would require optically-active low energy modes. Amorphous solids, with low-temperature specific heats revealing a spectrum of low-energy excitations (Pohl & Salinger 1976), are candidates for enhanced low-frequency absorption.

Laboratory measurements of the opacity of amorphous insulators are shown in Figure 1. In some cases (e.g., $\text{MgO} \cdot 2\text{SiO}_2$; Agladze et al. 1996) the submm opacity is consistent with a power law over the wavelength range studied. In other cases, broken power laws provide an acceptable fit. However, in all cases the power law index $\beta_s > 1$. The smallest effective value is $\beta_s \approx 1.2$ for $\text{MgO} \cdot 2\text{SiO}_2$ between 150 and 300 GHz (Agladze et al. 1996), but for most samples, $\beta_s \approx 2$, with $\beta_s > 2$ seen in some cases (e.g., $\text{Na}_2\text{O} \cdot 3\text{SiO}_2$ between 300 and 1200 GHz: Bösch 1978). While the number of materials studied is limited, it appears that small particles of amorphous insulators are likely to have $\beta_s \gtrsim 1.5$ in the submm.

For carbonaceous materials the situation is less clear. Opacities measured by Mennella et al. (1998) for materials “BE” (soot produced by burning C_6H_6 in air) and “ACAR” (amorphous

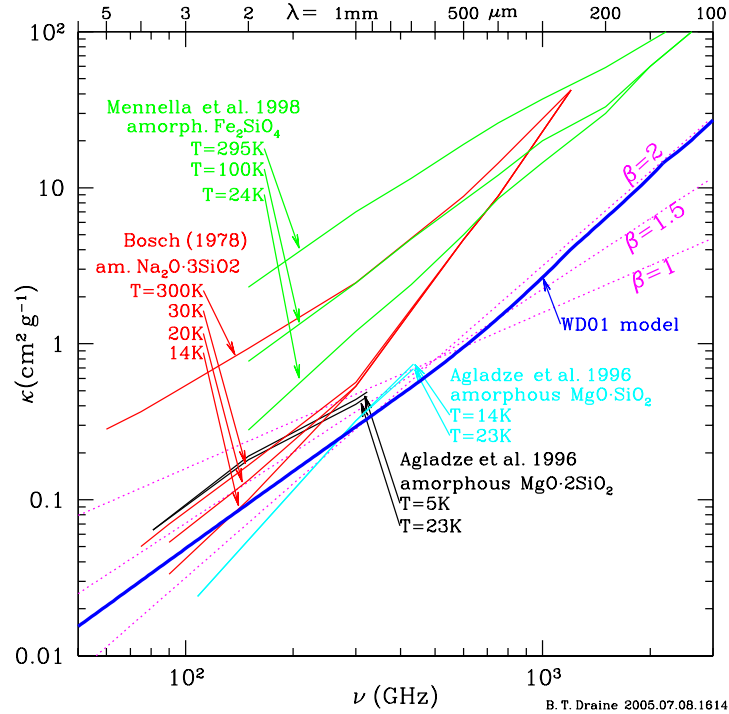


Fig. 1.— Laboratory measurements at various temperatures of opacities of amorphous Fe_2SiO_4 (Mennella et al. 1998), $\text{Na}_2\text{O} \cdot 3\text{SiO}_2$ (Bösch 1978), and $\text{MgO} \cdot 2\text{SiO}_2$ and $\text{MgO} \cdot \text{SiO}_2$ (Agladze et al. 1996). Curve labelled WD01 is the opacity of the Weingartner & Draine (2001) dust mixture, for comparison. Dotted lines show power laws with $\beta = 1$, 1.5, and 2.

carbon grains produced from a carbon arc in Ar gas) are shown in Figure 2. The opacities are very large (e.g., at 1mm, $\kappa \approx 25 - 30 \text{ cm}^2 \text{ g}^{-1}$ for BE and ACAR at 24K, a factor 20–100 larger than for the insulators in Fig. 1 at $T < 30\text{K}$). Samples BE and ACAR are characterized by small β_s : at 24K, BE and ACAR have $\beta_s \approx 1.1$ and 1.2, respectively. There is reason for concern that the very large submm opacities seen in the lab for materials BE and ACAR may be the result of contact between the particles in the sample (which could dramatically affect the opacity for materials with $|\epsilon| \gg 1$) in which case the measured opacities do not correspond to those that would be produced by isolated small spheres of the same material.

Jäger et al. (1999) have produced amorphous carbonaceous solids with varying levels of graphitization by pyrolysis of cellulose, and measured the optical constants. Pyrolysis at 600C in Ar gas produces a fine-grained material “cel600” with C:H:O::1:0.33:0.053 and density $\rho = 1.67 \text{ g cm}^{-3}$. Although the material is substantially “graphitized” (in the sense that $\sim 70\%$ of the C atoms appear to be sp^2 bonded, as in graphite), the material has $\epsilon_2 \rightarrow 0$ as $\nu \rightarrow 0$, implying zero d.c. conductivity. Jäger et al. provide the refractive index for $0.2\mu\text{m} < \lambda < 450\mu\text{m}$. We extrapolate to lower frequencies assuming $\epsilon_1(\lambda \geq 450\mu\text{m}) \approx 4.03$ and $\epsilon_2(\lambda \geq 450\mu\text{m}) = 0.0378(450\mu\text{m}/\lambda)^{0.3}$, giving $\beta_s = 1.3$ for $\lambda > 450\mu\text{m}$. The opacity calculated for small spheres of this material is shown in Figure 2. As noted by Jäger et al., small spheres have $\beta_s \approx 1.5$ for $\lambda \gtrsim 100\mu\text{m}$.

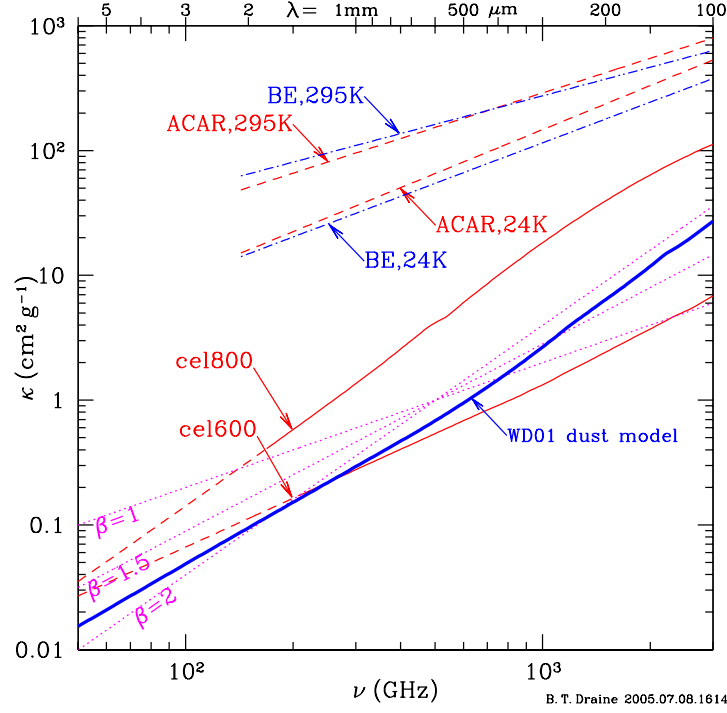


Fig. 2.— Same as Figure 1 but for carbonaceous materials BE and ACAR measured at $T = 24$ K and $T = 295$ K (Mennella et al. 1998), and calculated for small spheres with optical constants measured for cellulose pyrolyzed at 600C and 800C (Jäger et al. 1999) – see text.

Pyrolysis at 800C produces a material “cel800” with C:H:O::1:0.14:0.030, with $\rho = 1.84 \text{ g cm}^{-3}$ (Jäger et al. 1999). The estimated sp^2 fraction is $\sim 75\%$, and the material becomes conducting. Jäger et al. measured the optical constants for $0.178\mu\text{m} < \lambda < 562\mu\text{m}$; we extrapolate to lower frequencies with a simple free-electron model with conductivity $\sigma = 3.6 \times 10^{13} \text{ s}^{-1}$, and damping time $\tau = 1.5 \times 10^{-13} \text{ s}$. The opacity calculated for small spheres of cel800 is shown in Figure 2. At 1 mm, this calculated opacity is more than an order of magnitude below what was reported for ACAR and BE. As noted by Jäger et al., $\beta_s = 1.95$ for $\lambda > 100\mu\text{m}$.

With $|\epsilon| \gg 1$ in the submm, κ for cel800 is strongly shape-dependent. Because of its simple analytic properties, the “Continuous Distribution of Ellipsoids” (CDE) is sometimes used to allow for nonspherical shapes. Jäger et al. show that for the CDE, cel800 would have $\beta_s \approx 0.7$, but caution that the CDE serves only as an illustrative example of shape effects. The CDE assumes that a small fraction of the ellipsoids have very extreme shapes, and needle-like particles make a large contribution to κ when $|\epsilon| \gg 1$ (Min, Hovenier, & de Koter 2003). The shape distribution of interstellar particles does not seem likely to resemble the CDE, at least as regards these extreme shapes. We consider that spheres (or ellipsoids with modest axial ratios) provide a better approximation to interstellar particles than the CDE.

Any material capable of explaining $\beta \lesssim 1$ on the basis of composition rather than size would

have to be unlike the insulators in Figure 1, or the pyrolyzed cellulose in Figure 2. The opacities reported by Menella et al. for carbonaceous materials BE and ACAR are large and have $\beta \approx 1$, but it is not clear that the measured opacity would apply to free particles and, if it did, such material could not be a significant component of interstellar dust. Although one cannot exclude the possibility that protoplanetary disks might include material with both large mm/submm opacity and $\beta_s \approx 1$, alternate explanations should be considered.

3. Size Distribution

Consider particles with a power-law size distribution,

$$\frac{dn}{da} = A \left(\frac{a}{a_{\max}} \right)^{-p} \quad a_{\min} \leq a \leq a_{\max} \quad , \quad (3)$$

where A is a constant; the size distribution presumably results from competition between growth (e.g., coagulation) and destruction (e.g., shattering).

Experimental studies of fragmentation find power-law size distributions for the fragments, with p varying between ~ 1.9 for low-velocity collisions, to $p \approx 4$ for catastrophic impacts (Davis & Ryan 1990). However, the power-law index for fragments from shattering events integrated over a range of target masses need not be the same as the power-law index for fragments of a single target.

Dohnanyi (1969) showed that, for certain assumptions, coagulation and collisional fragmentation would lead to a steady-state size distribution with $p = 3.5$. Tanaka et al. (1996) argue that the $p = 3.5$ power law is in fact a very general result that depends *only* on the assumption that the fragmentation process is self-similar,¹ and that the collision rate varies as a^2 . Self-similarity may not apply to larger bodies, where self-gravity becomes important, or to the smallest sizes, where surface free energy considerations will limit the numbers of very small fragments, but self-similarity may apply, at least approximately, to the cratering and shattering events occurring in the interstellar medium and in protoplanetary disks.

Extinction and scattering of starlight by interstellar dust can be reproduced by a mixture of graphite and silicate grains with $p \approx 3.5$ and $a_{\max} \approx 0.25 \mu\text{m}$ (Mathis, Rumpl, & Nordsieck 1977; Draine & Lee 1984). Although more recent work (e.g., Kim & Martin 1995; Weingartner & Draine 2001) find deviations from a simple power law with cutoffs, the $p = 3.5$ power law gives a good accounting for the overall size distribution spanning many orders of magnitude in mass. While the origin of the interstellar grain size distribution remains uncertain, it is intriguingly close to the predictions of self-similar fragmentation.

The distribution of $D > 30$ km asteroids has $p \approx 3.4$ (Dohnanyi 1969). Based on observations by the Sloan Digital Sky Survey (Ivezić et al. 2001), the asteroid size distribution appears to be

¹If the collision rate varies as a^q , then $p = 2.5 + q/2$ (Tanaka et al. 1996).

consistent with $p \approx 3.25$ for diameters D between 5 and 300 km (Bottke et al. 2005).

If the size distribution of particles in a protoplanetary disk is determined by a competition between coagulation and fragmentation, it is plausible that the size distribution might be close to a power law with $p \approx 3.5$, with an upper cutoff a_{\max} that will depend on how far coagulation has proceeded. Note that for $p \approx 3.5$, most of the mass is at the large size end of the distribution, with the numbers of large grains nearly independent of the lower cutoff a_{\min} , provided $a_{\min} \ll a_{\max}$.

4. Analytic Approximation for the Opacity

For a size distribution dn/da , the opacity (absorption cross section per unit mass of solid materials) at frequency ν is given by

$$\kappa(\nu) \equiv \frac{\int da (dn/da) C_{\text{abs}}(a, \nu)}{\int da (dn/da) (4\pi/3) \rho a^3}, \quad (4)$$

where ρ is the solid density, and $a \equiv (3m/4\pi\rho)^{1/3}$ is the effective radius of a particle of mass m .

Consider some frequency ν , wavelength $\lambda = c/\nu$, and suppose that the absorption cross section for particles of size a can be approximated by

$$C_{\text{abs}}(a, \nu) \approx \begin{cases} (4\pi/3) a^3 \alpha_\nu & \text{for } a < a_c(\nu) \\ \pi a^2 & \text{for } a > a_c(\nu) \end{cases} \quad (5)$$

where

$$\alpha_\nu \equiv \frac{18\pi}{\lambda} \frac{\epsilon_2}{(\epsilon_1 + 2)^2 + \epsilon_2^2} \quad \text{and} \quad a_c \equiv \frac{3}{4\alpha_\nu} \equiv \frac{\lambda}{24\pi} \frac{(\epsilon_1 + 2)^2 + \epsilon_2^2}{\epsilon_2} \quad (6)$$

are defined so that eq. (5) is exact for spheres in the small particle limit ($a/\lambda \rightarrow 0$) (see, e.g., Draine & Lee 1984). Here $\epsilon_1(\lambda)$ and $\epsilon_2(\lambda)$ are the real and imaginary parts of the complex dielectric function $\epsilon \equiv \epsilon_1 + i\epsilon_2$. Eq. (5) is only approximate for $a \gtrsim \lambda/2\pi$, but the limiting behavior in the geometric optics limit $a \rightarrow \infty$ is sensible, corresponding to a low-albedo object. Because we will be interested in size distributions where the surface area is dominated by small particles, our analytic estimate of the opacity integral (4) is relatively insensitive to errors in the albedo of the particles with $a \gg \lambda/2\pi$. For $a \approx \lambda/2\pi$, C_{abs} can exceed eq. (5) by as much as a factor ~ 10 (depending on ϵ), but for the moment we use eq. (5) to estimate the opacity for the size distribution (3):

$$\kappa(\nu) = \frac{\alpha_\nu}{\rho} \quad \text{if } a_{\max} < a_c \quad (7)$$

and

$$\kappa(\nu) = \frac{\alpha_\nu}{\rho} \frac{1}{(p-3)} \left(\frac{a_c}{a_{\max}} \right)^{4-p} \left[1 - (p-3) \left(\frac{a_{\min}}{a_c} \right)^{4-p} - (4-p) \left(\frac{a_{\max}}{a_c} \right)^{3-p} \right] \quad (8)$$

for $a_{\min} < a_c < a_{\max}$, $p > 3$, $p \neq 4$, and $a_{\min} \ll a_{\max}$. If $3 < p < 4$, then

$$\kappa(\nu) \approx \frac{3}{4\rho a_{\max}} \frac{1}{(p-3)} \left(\frac{4\alpha_\nu a_{\max}}{3} \right)^{p-3} \quad \text{if } a_{\min} \ll a_c \ll a_{\max} \quad (9)$$

If the small-particle absorption cross section per volume varies as a power-law in frequency,

$$\alpha_\nu = \alpha_0 \left(\frac{\nu}{\nu_0} \right)^{\beta_s}, \quad (10)$$

then

$$\kappa(\nu) = \frac{\alpha_0}{(p-3)\rho} \left(\frac{3}{4\alpha_0 a_{\max}} \right)^{4-p} \left(\frac{\nu}{\nu_0} \right)^{(p-3)\beta_s} \quad \text{if } a_{\min} \ll a_c \ll a_{\max} \quad . \quad (11)$$

Therefore, if $a_{\min} \ll a_c \ll a_{\max}$, the size distribution will have

$$\beta \approx (p-3)\beta_s \quad . \quad (12)$$

For $p = 3.5$ and $\beta_s \approx 1.7$, eq. (12) predicts $\beta \approx 0.85$: material with the FIR-submm opacity characteristic of diffuse interstellar dust ($\beta_s \approx 1.7$) can reproduce the observed frequency dependence of the opacity of material in circumstellar disks ($\beta_{\text{disk}} \approx 1$) if a_{\max} is large enough so that $a_{\max} \gg a_c(\lambda)$ over the frequency range of interest.

The derivation of eq. (11-12) relied on the approximations (5), which are known to not be quantitatively accurate. We now proceed to direct calculation of $\kappa(\nu)$ for several candidate materials to determine the actual frequency dependence of β , and to see what values of κ result when a_{\max} is large enough to satisfy the condition (9).

5. Examples

The precise behavior of $\kappa(\nu)$ depends on the complex dielectric function $\epsilon(\nu)$. Not knowing the precise composition of interstellar and protostellar grain material, we consider three, quite different, candidate materials. We will see that for the different materials considered here, a power-law size distribution with $p \approx 3.5$ results in mm/submm opacities with $\beta \approx 0.9$ provided $a_{\max} \gtrsim 3$ mm.

The opacity $\kappa(\nu)$ (eq. 4) is evaluated with $C_{\text{abs}}(a, \nu)$ calculated for spheres, using Mie theory for $a < a_x \equiv 2 \times 10^4 \lambda / 2\pi |m|$, and geometric optics for $a > a_x$, where $m = \sqrt{\epsilon}$ is the complex refractive index. We employ a double precision version of the Mie theory implementation of Wiscombe (1980, 1996).

5.1. Silicate Particles

We calculate the opacity of spherical silicate particles using the dielectric function estimated for interstellar silicate material (Draine 2003). Figure 3 shows $\kappa(\nu)$ for size distributions with $p = 3.5$, $a_{\min} = 3.5 \text{ \AA}$, and various values of a_{\max} . The curve labelled $0.25 \mu\text{m}$ is the “small particle” opacity estimated for interstellar silicate grains. At $\lambda = 1$ mm, increasing a_{\max} does not noticeably change the opacity until a_{\max} reaches $100 \mu\text{m}$, at which point the optics of small particles with $2\pi a/\lambda \approx 1$ results in an *increase* in the opacity. This effect leads to opacities for the

overall size distribution that *exceed* the small-particle opacity at 1 mm until a_{\max} reaches 10 cm. For $a_{\max} \gtrsim 1$ mm, $\kappa(1 \text{ mm}) \propto 1/\sqrt{a_{\max}}$, consistent with eq. (11). The upper panel in Fig. 3 shows the opacity spectral index $\beta(\lambda)$ for the different choices of a_{\max} . For this material, the condition $a_c \ll a_{\max}$ can be replaced by $3\lambda \lesssim a_{\max}$. We see that $\beta(1 \text{ mm}) \lesssim 1$ for $a_{\max} \gtrsim 3$ mm.

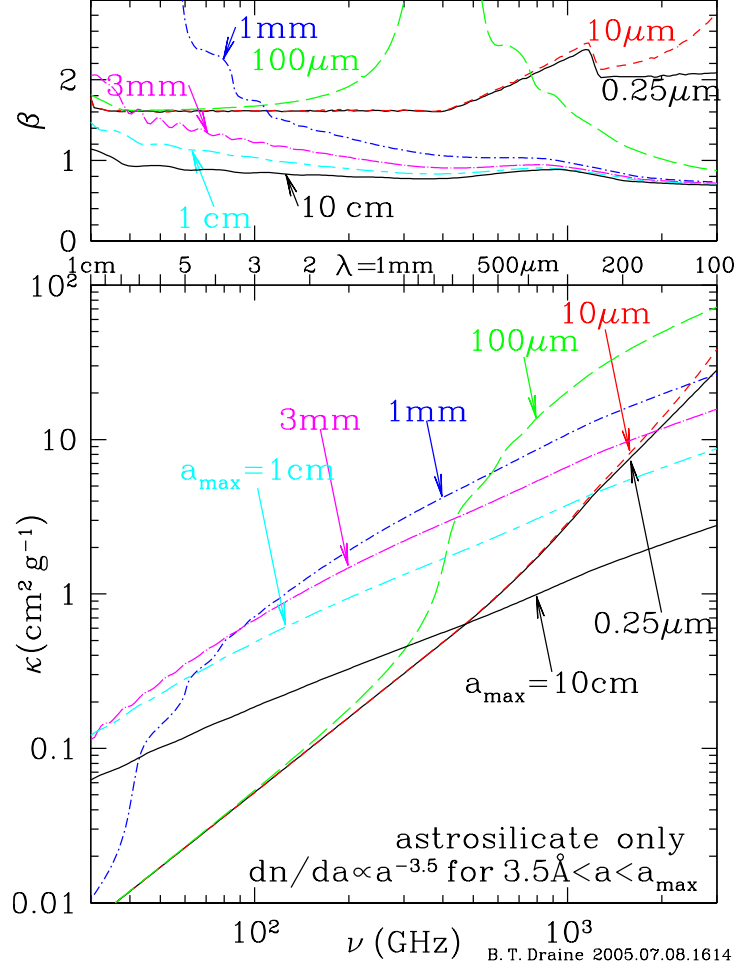


Fig. 3.— Opacity of amorphous silicate spheres with size distribution $dn/da \propto a^{-3.5}$ for $3.5 \text{ \AA} < a < a_{\max}$. Curves are labelled by a_{\max} ; curve for $0.25 \mu\text{m}$ is the small-particle limit, and numerically close to the WD01 dust model (not shown). Upper panel shows $\beta \equiv d \ln \kappa / d \ln \nu$ for selected a_{\max} . $\beta(1 \text{ mm}) \lesssim 1$ is found for $a_{\max} \gtrsim 3$ mm.

5.2. Amorphous Carbonaceous Material

The dust model of Weingartner & Draine (2001; hereafter WD01) includes carbonaceous material with the anisotropic dielectric function of graphite, with absorption and scattering by randomly-oriented spherical grains estimated using the “1/3-2/3 approximation” (Draine & Malhotra 1993).

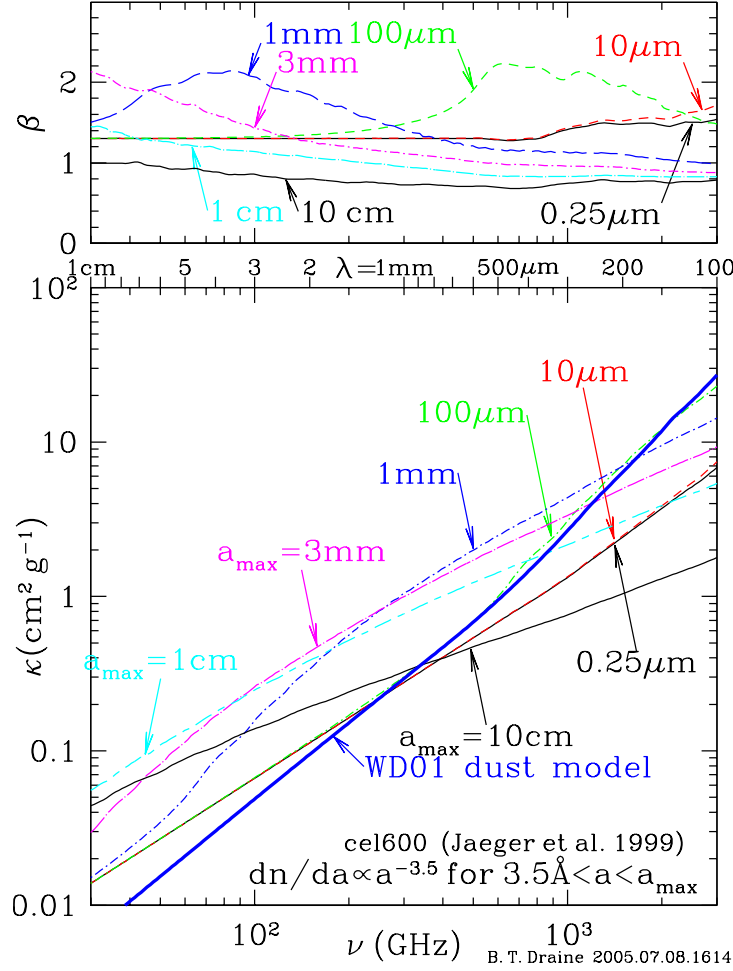


Fig. 4.— Same as Fig. 3, but using the optical constants of cellulose pyrolyzed at 600C (Jäger et al. 1999). Also shown is the opacity for the WD01 dust model. For $a_{\text{max}} \leq 100 \mu\text{m}$, $\kappa(1 \text{ mm})$ is very similar to the WD01 opacity. For $a_{\text{max}} \gtrsim 3 \text{ mm}$, the opacity has $\beta(1 \text{ mm}) \lesssim 1$.

Graphite is a conductor, with appreciable conductivity in the basal plane, and nonzero electrical conductivity even parallel to the c axis (i.e., normal to the basal plane). For large particles at submm wavelengths, the conductivity plays a major role in determining the absorption cross section. Because large particles formed by coagulation will not have the properties of crystalline graphite, we consider instead the amorphous carbonaceous solids cel600 and cel800 studied by Jäger et al. (1999) (see §2).

Figure 4 shows the FIR-submm opacity for size distributions of cel600 spheres. In the small-particle limit, the opacity of cel600 near $\lambda = 1 \text{ mm}$ is similar to or less than the opacity of the WD01 grain model, and at $100 \mu\text{m}$ the opacity is less than the WD01 model by a factor ~ 3 . The WD01 model successfully reproduces the observed emission from the ISM (Li & Draine 2001) and other

spiral galaxies (Regan et al. 2004). Candidate interstellar grain materials that do not substantially exceed the WD01 opacity could, in principle, be abundant in the ISM. Thus, the mm/submm properties of interstellar carbonaceous material could perhaps resemble cel600. The mm/submm opacity of the size distributions of cel600 is insensitive to a_{\max} until a_{\max} reaches $\sim 100\mu\text{m}$. Size distributions of cel600 with $p = 3.5$ have $\beta(1\text{ mm}) \lesssim 1$ for $a_{\max} \gtrsim 1\text{ cm}$.

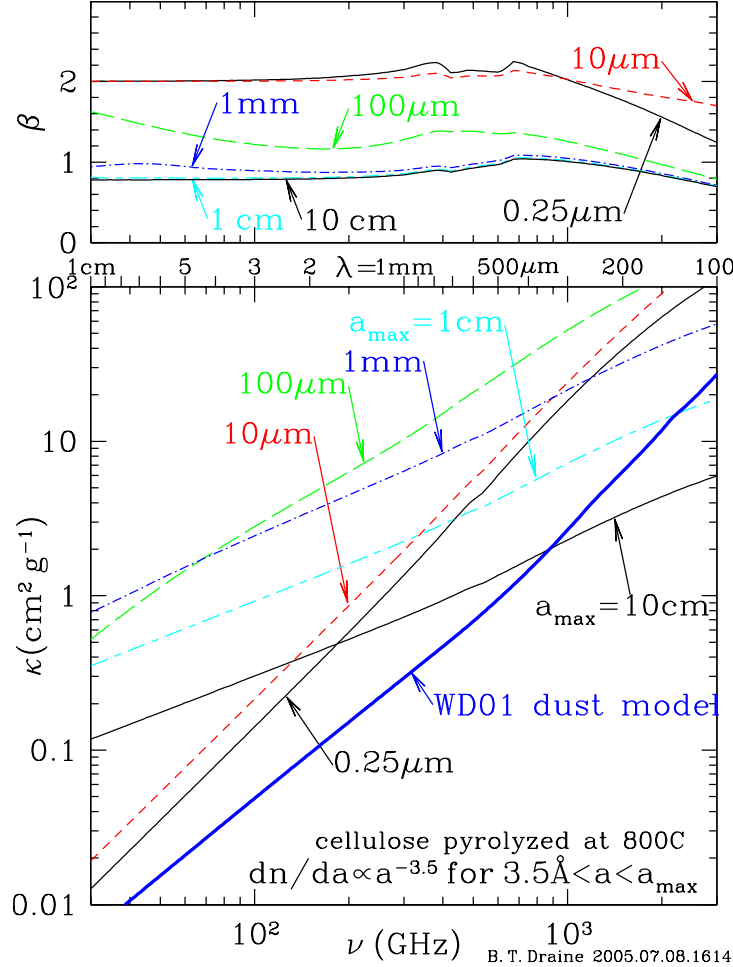


Fig. 5.— Same as Fig. 4, but for cellulose pyrolyzed at 800C (Jäger et al. 1999), resulting in a material with appreciable d.c. conductivity. In this case, magnetic dipole absorption (see text) causes $\kappa(\lambda = 1\text{ mm})$ to increase as a_{\max} is increased beyond $1\mu\text{m}$. These particles have $\beta(1\text{ mm}) < 1.2$ for $a_{\max} \gtrsim 200\mu\text{m}$.

Spheres composed of cel800, on the other hand, gives FIR and submm absorption that is much stronger than in the WD01 dust model, even when the material is in the form of spheres – any other shape would provide even stronger absorption. For $1\text{ mm} \lesssim \lambda \lesssim 100\mu\text{m}$, in the small-particle limit κ exceeds the WD01 opacity by factors of ~ 4 ; hence it does not seem likely that the interstellar grain mix could include very much such material. Nevertheless, because we cannot rule out the possibility that protoplanetary disk material might have optical properties resembling cel800, we consider size distributions of spheres composed of cel800 as an example of a conducting

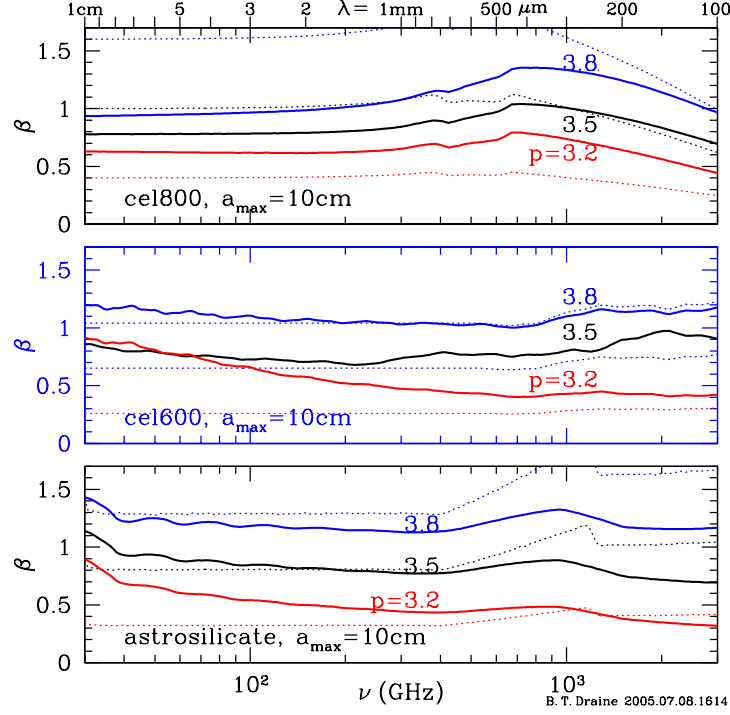


Fig. 6.— $\beta(\nu)$ for size distributions $dn/da \propto a^{-p}$, for 3 values of p , and the materials of Figs. 3–5. Dotted lines are $(p - 3)\beta_s$, which should be approximately equal to $\beta(\lambda)$ (see eq. 12), for $p = 3.2, 3.5, 3.8$ (bottom to top in each panel) showing approximate agreement with the actual β values.

material. In the small-particle limit, cel800 has $\beta_s \approx 2$, but size distributions with $a_{\max} \gtrsim 3$ mm give $\beta(1 \text{ mm}) \approx 0.9$, showing the generality of the result (12).

To see the sensitivity of β to the power-law index p , Fig. 6 shows β for $p = 3.2, 3.5$, and 3.8 . The opacity spectral index $\beta(1 \text{ mm}) < 1$ requires $p \lesssim 3.6$ for astrosilicate or cel600, or $p \lesssim 3.8$ for cel800.

The relation $\beta \approx (p - 3)\beta_s$ was derived using eq. (5), which is not an accurate approximation for C_{abs} when $a \gtrsim \lambda/2\pi$. Also shown in Fig. 6 (dotted lines) are $(p - 3)\beta_s(\nu)$ for $p = 3.2, 3.5$, and 3.8 . We see that while $(p - 3)\beta_s$ is often close to the actual $\beta(\nu)$, there are regimes where β differs appreciably from this estimate (e.g., astrosilicate with $p = 3.8$ at $\nu > 10^3$ GHz; cel600 with $p = 3.2$ for $\nu < 10^2$ GHz, and cel800 with $p = 3.8$ for $\nu < 500$ GHz). Nevertheless eq. (12) provides a reasonable estimate.

6. Discussion

6.1. Ices?

In diffuse clouds, H_2O and other ices are not detected: ultraviolet radiation prevents the accumulation of H_2O ice coatings on grains in diffuse clouds. In dark clouds, however, substantial amounts of solids containing H_2O , CO , CH_3OH , H_2CO , NH_3 , CH_4 , and other compounds are observed to be present, presumably as “mantles” coating “cores” (silicate and carbonaceous material) inherited from diffuse clouds.

What will be the role of these ices at submm wavelengths? Using the dielectric function of crystalline H_2O ice I, Aannestad (1975) found that the presence of ice mantles had only minor effects on the absorption at $\lambda \gtrsim 200\mu\text{m}$, because the vibrational and hindered-rotation modes of the H_2O all lie at higher frequencies. This is confirmed in recent work (Pontoppidan et al. 2005).

Preibisch et al. (1993) considered silicate grains coated with “dirty ice” consisting of a mixture of H_2O and NH_3 with small amorphous carbon inclusions. The optical properties of this mixture were estimated using effective medium theory. In the submm, the absorption by this “dirty ice” material was almost entirely due to the amorphous carbon inclusions. When present as inclusions within an ice matrix, the amorphous carbon material is more absorptive than when present as a bare particle. It should be kept in mind, however, that this conclusion is based on use of approximate effective medium theories to estimate the optical properties of the ice with inclusions.

Therefore, although the absorption cross section for a silicate or carbonaceous grain will change if an ice mantle develops on the grain, at submm frequencies it does not appear that this will substantially alter the grain absorption cross section unless the ice itself is strongly absorbing, and strong absorption does not appear likely unless the “ice” is contaminated by amorphous carbon particles – in which case the absorption is due to the amorphous carbon, not the ice itself.

6.2. Grain Growth

Beckwith & Sargent (1991) suggested that grain growth might explain the values of $\beta_{\text{disk}} \approx 1$ inferred from their observations. Miyaka & Nakagawa (1993) calculated the opacity for size distributions extending to $a_{\text{max}} \gtrsim 1\text{ cm}$, and concluded that grain growth could indeed account for the observed values of β_{disk} . Miyaka & Nakagawa considered grains composed of mixtures of silicate and H_2O ice, either as compact solids or in fluffy structures. The present paper shows that the result of Miyaka & Nakagawa is quite general, and applies to both conducting and nonconducting materials.

D’Alessio et al. (2001) calculated the opacity for power-law size distributions with $p = 2.5$ and $p = 3.5$, for a mixture of separate spheres of silicate, ice, and organic material, but for the silicate material they assumed constant ϵ_2 for $\lambda > 800\mu\text{m}$, resulting in $\beta_s = 1$ for the silicate spheres at

$\lambda > 800\mu\text{m}$. Therefore even in the small particle limit, their model had $\beta_s = 1$ for $\lambda > 800\mu\text{m}$. This frequency dependence is not expected – see Fig. 1 where amorphous insulators have $\beta_s \approx 2$ at mm wavelengths.

Natta et al. (2004) calculated κ and β for power-law size distributions with various exponents p for mixtures of compact spheres of olivine, organic material, and water ice, and also for fluffy grains containing mixtures of the above, with 50% vacuum. They used dielectric functions such that $\beta_s = 1.27$ for the mixture of separate, compact spheres (Natta & Testi 2004). They showed that by increasing a_{max} to $a_{\text{max}} \gtrsim 3\text{ mm}$ for the compact grains, or $a_{\text{max}} \gtrsim 10\text{ cm}$ for the fluffy grains, size distributions with $p \approx 3.5$ would have $\beta(1\text{ mm}) \approx 1$.

The results of the present paper are in general agreement with these previous studies. We also point out that when $a_{\text{max}} \gtrsim \lambda$, the approximate estimate $\beta \approx (p - 3)\beta_s$ applies to both insulating and conducting particles (for $3 < p < 4$). For the likely power-law index $p \approx 3.5$, this gives $\beta \approx 0.5\beta_s$, so that materials with $\beta_s = 2$, for example, are expected to have $\beta \approx 1$ when $a_{\text{max}} \gg \lambda$. Direct calculation of κ for size distributions of three candidate materials – silicate, nonconducting carbonaceous material (cel600), and conducting carbonaceous material (cel800) confirm that power-law size distributions with $p \approx 3.5$ will have $\beta \lesssim 1$ for $a_{\text{max}} \gtrsim 3\lambda$.

It is sometimes suggested that the low values of β_{disk} are due to “fluffiness” of grains grown by agglomeration (Beckwith & Sargent 1992). Fluffiness could substantially increase the mm/submm opacity if the grain material is electrically conducting (Wright 1987), but for nonconducting materials with dielectric functions that are not very large at the wavelengths of interest, grain geometry will have only modest effects on the grain opacity. Krügel & Siebenmorgen (1994) considered extinction and absorption by “fluffy” grains composed of silicate, amorphous carbon, and ice. The absorptivity of the ice in the far infrared was treated as a free parameter, and chosen to be large enough for the ice absorption to dominate the submm absorption. With their adopted optical constants, the particles had $\beta_s \approx 1.8$ for $\lambda > 100\mu\text{m}$. They found that power-law size distributions (3) with $p = 3.5$ and $a_{\text{max}} = 3\text{ mm}$ had $\beta \approx 0.5$ for $100\mu\text{m} \lesssim \lambda \lesssim 2\text{ mm}$.

Stognienko et al. (1995) discussed the optical properties of particles produced by coagulation of smaller sub-particles, and showed that the opacity of such clusters depends strongly on the optical properties of the sub-particles, and on the geometry of the clustering. For amorphous carbon sub-particles, the particle geometry can lead to strong enhancements in absorption for some cluster topologies. However, if the cluster size $a \ll \lambda$, the clusters appear to have $\beta \approx 2$ at submm frequencies. Henning & Stognienko (1996) calculated the opacity for dust aggregates; their standard model has $\beta \approx 2$ for the aggregates.

From the above studies we conclude that, while grain structure unquestionably plays a role in determining scattering and absorption cross sections, the observed small values of β_{disk} are naturally explained simply as the result of increased grain size, independent of whether the grains are compact or conglomerate. Grain growth to sizes $\gtrsim 3\text{ mm}$ can naturally account for the observed $\beta_{\text{disk}}(1\text{ mm}) \approx 1$.

7. Summary

The principal conclusion of this paper is the following: if the solid particles in protostellar disks have size distributions $dn/da \propto a^{-p}$ for $a < a_{\max}$, with $p \approx 3.5$ (as observed for interstellar dust, and as seems likely for particles in protoplanetary disks) and $a_{\max} \gtrsim 3$ mm, the resulting opacities have $\beta(1 \text{ mm}) \approx (p - 3)\beta_s \approx 1$, where β_s is the opacity spectral index in the small particle limit. Therefore if the particles in protoplanetary disks are composed of the same material as interstellar grains (with $\beta_s \approx 1.8 \pm 0.2$ in the submm) and the size distribution has $p \approx 3.5$ and extends to $a_{\max} \gtrsim 3$ mm, the protoplanetary disk material will have $\beta(1 \text{ mm}) \lesssim 1$. This result is not expected to be altered by the addition of dielectric ice coatings on the grains.

To demonstrate the generality of this conclusion, three quite different materials were considered: two amorphous insulators (astrosilicate and cellulose pyrolyzed at 600C) and a conductor (cellulose pyrolyzed at 800C). While the relation $\beta \approx (p - 3)\beta_s$ is only an approximation, we find that all 3 materials give $\beta(1 \text{ mm}) \lesssim 1$ for $p \approx 3.5$ and $a_{\max} \gtrsim 3$ mm.

The observed submm emission from protostellar disks therefore is explained naturally by the particle growth that is expected to occur in these disks.

This research was supported in part by NSF grant AST-0406883. I am grateful to A. Natta for helpful discussions, and to R.H. Lupton for availability of the SM software package.

REFERENCES

- Aannestad, P.A. 1975, *ApJ*, 200, 30
- Agladze, N.I., Sievers, A.J., Jones, S.A., Burlitch, J.M., & Beckwith, S.V.W. 1996, *ApJ*, 462, 1026
- Andrews, S.M., & Williams, J.P. 2005, *ApJ*, accepted [astro-ph/0506187v1]
- Beckwith, S.V.W., Henning, Th., & Nakagawa, Y. 2000, in *Protostars and Planets IV*, ed. V. Mannings, A.P. Boss, & S.S. Russell, (Tucson: U. of Arizona Press), p. 533.
- Beckwith, S.V.W., & Sargent, A.I. 1991, *ApJ*, 381, 250
- Beuther, H., Hunter, T.R., Zhang, Q., Sridharan, T.K., Zhao, J.-H., Sollins, P., Ho, P.T.P., Ohashi, N., Su, Y.N., Lim, J., & Liu, S.-Y. 2005, *ApJ*, 616, L23
- Bösch, M.A. 1978, *Phys. Rev. Lett.*, 40, 879
- Bottke, W.F., Jr., Durda, D.D., Nesvorný, D., Jedicke, R., Morbidelli, A., Vokrouhlický, D., & Levison, H. 2005, *Icarus*, 175, 111
- D'Alessio, P., Calvet, N., & Hartmann, L. 2001, *ApJ*, 553, 221

- Davis, D.R., & Ryan, E.V. 1990, *Icarus*, 83, 156
- Dohnanyi, J.W. 1969, *JGR*, 74, 2531
- Draine, B.T. 2003, *ApJ*, 598, 1026
- Draine, B.T. 2004, in *The Cold Universe*, Saas-Fee Advanced Course 32, ed. D. Pfenniger & Y. Revaz (Berlin: Springer-Verlag), p. 213
- Draine, B.T., & Lee, H.-M. 1984, *ApJ*, 285, 89
- Draine, B.T., & Malhotra, S. 1993, *ApJ*, 414, 632
- Dullemond, C.P., & Dominik, C. 2005, *A&A*, 434, 971
- Finkbeiner, D.P., Davis, M., & Schlegel, D.J. 1999, *ApJ*, 524, 867
- Friesen, R.K., Johnstone, D., Naylor, D.A., & Davis, G.R. 2005, *MNRAS*, 000, 000 (astro-ph/0505331v1).
- Goldsmith, P.F., Bergin, E.A., & Lis, D.C. 1997, *ApJ*, 491, 615
- Henning, Th., & Stognienko, R. 1996, *A&A*, 311, 291
- Hunter, T.R. 1998, *PASP*, 110, 634
- Ivezić, Z., et al. 2001, *AJ*, 122, 2749
- Jäger, C., Mutschke, H., & Henning, Th. 1998, *A&A*, 332, 291
- Kim, S.-H., & Martin, P.G. 1995, *ApJ*, 444, 293
- Krügel, E., & Siebenmorgen, R. 1994, *A&A*, 288, 929
- Li, A., & Draine, B.T. 2001, *ApJ*, 554, 778
- Mathis, J.S., Rumpl, W., & Nordsieck, K.H. 1977, *ApJ*, 217, 425
- Mennella, V., Brucato, J.R., Colangeli, L., Palumbo, P., Rotundi, A., & Bussoletti, E. 1998, *ApJ*, 496, 1058
- Min, M., Hovenier, J.W., & de Koter, A. 2003, *A&A*, 404, 35.
- Miyake, K., & Nakagawa, Y. 1993, *Icarus*, 106, 20
- Natta, A., & Testi, L. 2004, in *Star Formation in the Interstellar Medium*, ed. D. Johnstone, F.C. Adams, D.N.C. Lin, D.A. Neufeld, & E.C. Ostriker, ASP Conf. Series, 323, 279
- Natta, A., Testi, L., Neri, R., Shepherd, D.S., & Wilner, D.J. 2004, *A&A* 416, 179

- Pohl, R.O., & Salinger, G.L. 1976, *Ann. N.Y. Acad. Sci.*, 279, 150
- Pontoppidan, K.M., Dullemond, C.P, van Dishoeck, E.F., Blake, G.A., Boogert, A.C.A., Evans, N.J., Kessler-Silacci, J.E., & Lahuis. F. 2005, *ApJ*, 622, 463
- Preibisch, Th., Ossenkopf, V., Yorke, H.W., & Henning, Th. 1993, *A&A*, 279, 577
- Regan, M.W., Thornley, M.D., Bendo, G., Draine, B.T., Li, A., Dale, D.A., Engelbracht, C.W., et al. 2004, *ApJS*, 154, 199
- Stognienko, R., Henning, Th., & Ossenkopf, V. 1995, *A&A*, 296, 797
- Tanaka, H., Inaba, S., & Nakazawa, K. 1996, *Icarus*, 123, 450
- Weingartner, J.C., & Draine, B.T. 2001, *ApJ*, 548, 296 (WD01)
- Wiscombe, W.J. 1980, *Appl. Opt.*, 19, 1505
- Wiscombe, W.J. 1996, NCAR Technical Note NCAR/TN-140+STR, ftp://climate.gsfc.nasa.gov/pub/wiscombe/Single-Scatt/Homogen_Sphere/Exact_Mie/NCARMieReport.pdf
- Wright, E.L. 1987, *ApJ*, 320, 818